Article

Important Role of Asparagines in Coupling the Pore and Votage-Sensor Domain in Voltage-Gated Sodium Channels

Michael F. Sheets,[1,*] Harry A. Fozzard,[2] and Dorothy A. Hanck[2]
[1]Nora Eccles Harrison Cardiovascular Research and Training Institute (CVRTI), University of Utah, Salt Lake City, Utah; and [2]University of Chicago, Chicago, Illinois

ABSTRACT Voltage-gated sodium (Na_V) channels contain an α-subunit incorporating the channel's pore and gating machinery composed of four homologous domains (DI–DIV), with a pore domain formed by the S5 and S6 segments and a voltage-sensor domain formed by the S1–S4 segments. During a membrane depolarization movement, the S4s in the voltage-sensor domains exert downstream effects on the S6 segments to control ionic conductance through the pore domain. We used lidocaine, a local anesthetic and antiarrhythmic drug, to probe the role of conserved Asn residues in the S6s of DIII and DIV in $Na_V1.5$ and $Na_V1.4$. Previous studies have shown that lidocaine binding to the pore domain causes a decrease in the maximum gating (Q_{max}) charge of ~38%, and three-fourths of this decrease results from the complete stabilization of DIII-S4 (contributing a 30% reduction in Q_{max}) and one-fourth is due to partial stabilization of DIV-S4 (a reduction of 8–10%). Even though substitutions for the Asn in DIV-S6 in $Na_V1.5$, N1764A and N1764C, produce little ionic current in transfected mammalian cells, they both express robust gating currents. Anthopleurin-A toxin, which inhibits movement of DIV-S4, still reduced Q_{max} by nearly 30%, a value similar to that observed in wild-type channels, in both N1764A and N1764C. By applying lidocaine and measuring the gating currents, we demonstrated that Asn residues in the S6s of DIII and DIV are important for coupling their pore domains to their voltage-sensor domains, and that Ala and Cys substitutions for Asn in both S6s result in uncoupling of the pore domains from their voltage-sensor domains. Similar observations were made for $Na_V1.4$, although substitutions for Asn in DIII-S6 showed somewhat less uncoupling.

INTRODUCTION

Voltage-gated sodium (Na_V) channels are responsible for the rapid conduction velocities of action potentials in excitable tissues such as nerves and cardiac muscle, and thus are therapeutic targets for seizure disorders, pain syndromes, and cardiac arrhythmias. The ~2000 amino acid Na channel α-subunit contains the channel's pore and gating machinery, and all of the drug and toxin interaction sites identified to date (1). It has four homologous domains (DI–DIV) and is thought to be analogous to the K channel's four separate subunits, which contain a pore domain formed by the S5 and S6 segments and a voltage-sensor domain formed by S1–S4 segments located toward the periphery of the channel (2,3). Ionic currents are elicited in response to changes in the membrane potential sensed by the channel's voltage-sensor domains, which are coupled to its pore domain.

A critical feature of local anesthetic and antiarrhythmic (LA) drugs is their dramatic voltage-dependent binding to the internal pore of Na_V, which blocks ion permeation. This voltage dependence is determined by an interaction between the voltage sensors and the channel gates formed by S6 segments that also form the pore and the LA-binding site (4–7). Binding of lidocaine, an LA drug, to the inner pore of wild-type (WT) human cardiac $Na_V1.5$ channels causes a decrease in the maximum gating (Q_{max}) charge of nearly 38–40% (8). Three-fourths of this decrease results from the complete stabilization of DIII-S4 (contributing to a 30% reduction in Q_{max}) and one-fourth is due to partial stabilization of DIV-S4 (a reduction of ~10%) (8). Furthermore, the partial stabilization of DIV-S4 by lidocaine causes its remaining gating charge to move at more negative potentials, resulting in an excess gating charge of approximately −100 mV compared with WT channels (8,9). Muroi and Chanda (10) obtained comparable results regarding the action of local anesthetic drugs for the S4s in DIII and DIV by measuring shifts in the fluorescence-voltage curves of the S4s in the rat skeletal muscle Na channel, $rNa_V1.4$.

The coupling of the pore domain to the voltage-sensor domain has been shown to result from interactions between the S4-S5 linkers, the S6 segments, and the voltage sensors formed by the S4s in voltage-gated K channels (3). In addition, studies have shown a specific coupling of the outer pore of the Na channel to the voltage sensor in DIV that may be involved in slow inactivation (11). The residues responsible for coupling the pore domain to the voltage-sensor domains of the Na_V channel remain incompletely understood. Two previous studies used tryptophan scanning of ~55 residues in the S4-S5 linker and the S5 and S6 helices of DIII in $rNa_V1.4$ expressed in *Xenopus* oocytes to measure

Submitted July 2, 2015, and accepted for publication October 8, 2015.
*Correspondence: michael@cvrti.utah.edu
Editor: Randall Rasmusson.

0006-3495/15/12/2277/10
http://dx.doi.org/10.1016/j.bpj.2015.10.012

shifts in the fluorescence-voltage curves of DIII-S4, but substitution for N1281 was found to be generally unremarkable (12,13). However, a study using Cys scanning in DIV-S6 in rNa$_V$1.4 found that the I_{Na} resulting from the substitution of a Cys for Asn (N1584C) was too small for routine measurement (14). Similar small magnitudes of I_{Na} were found for N1584A mutations in rNa$_V$1.4 channels, again suggesting that the mutant did not express well or the expressed channels had a marked reduction in ionic current (15).

Using lidocaine and the site-3 toxin Anthopleurin-A (ApA), both of which have well-described actions on the gating of WT Na$_V$1.5, we investigated the role of the highly conserved Asn residues in the S6s of DIII and DIV, and their role in coupling the pore domain to the voltage-sensor domain. Table 1 shows the Asn residues in each of the S6s (N406, N932, N1462, and N1764; numbering based on hH1a (16)) are located at similar positions that have been modeled to be two residues inward from the putative bundle crossing in Na$_V$1.5 (6). In contrast to the very small I_{Na} magnitudes obtained from both Ala (N1764A) and Cys (N1764C) substitutions for the Asn in DIV-S6, we found that the two mutant channels expressed as well as or better than the WT channels in mammalian cells as measured by the presence of gating currents. Moreover, similar to the case with the WT, the voltage-dependent movement of DIV-S4 in both N1764C and N1764A was modified by ApA toxin, i.e., toxin stabilized DIV-S4 movement similarly to WT Na$_V$1.5-S4 (17–20), suggesting that the substitutions for Asn did not stabilize DIV-S4. By applying lidocaine and measuring the gating currents, we demonstrated that Asn residues in the S6s of DIII and DIV are important for coupling the pore domains to the voltage-sensor domains, and that Ala and Cys substitutions for Asn in both S6s result in uncoupling of the pore domains from their voltage-sensor domains.

MATERIALS AND METHODS

Molecular constructs

Four-primer PCR (21,22) or QuikChange (Agilent Technologies, Santa Clara, CA) was used to substitute site-directed Ala or Cys residues for the native Asn in human Na$_V$1.5 (cDNA for hH1a was kindly provided by H. Hartmann and A. Brown) (23) or the rat skeletal muscle rNa$_V$1.4 channel. In Na$_V$1.5 (using the numbering system of hH1a (16)), the Asn residues in the S6s of DIII (N1462) and DIV (N1764) in Na$_V$1.5, and the corresponding Asn residues in the S6s of DIII (N1281) and DIV (N1584) in rNa$_V$1.4, were mutated (24). The entire inserts containing the mutated sites were confirmed by sequencing. In addition, all constructs of Na$_V$1.5 contained a Tyr substituted for the Cys in the external vestibule of the pore at position 373 (C373Y) to increase the sensitivity to block by saxitoxin (STX) (25). For expression in mammalian cells, the cDNAs were subcloned directionally into the mammalian expression vector pRc/CMV or pcDNA (Invitrogen, Carlsbad, CA). The β1 subunit (26) was subcloned directionally into pRcCMV (27).

TABLE 1 Inner-pore (intracellular) sequences of S6 segments in human Na$_V$1.5

I	S	F	Y	L	V	**N**	L	I	L	A	V	V	A	M
II	G	N	L	V	V	L	**N**	L	F	L	A	L	L	L
III	G	S	F	F	T	L	**N**	L	F	I	G	V	I	I
IV	S	F	L	I	V	V	**N**	M	Y	I	A	I	W	I	L

Asn (N) residues are in boldface. The sequences are conserved in rat Na$_V$1.4 except that the first Val is an Ile in DI.

Cell preparation

Single tsA201 cells (SV40 transformed HEK293 cells) were fused as previously described (28), with the following changes: tsA201 cells were grown on 100 mm petri dishes until they reached ~95% confluency. Four hours after the addition of fresh standard media (Dulbecco's modified Eagle's medium (DMEM; Sigma-Aldrich, St. Louis, MO) supplemented with 10% fetal bovine serum and 1% penicillin/streptomycin), the plate was washed with media containing only DMEM. A cell fusion solution was made from PEG1450 (2.0 gm/vial; ATCC, Manassas, VA) with the addition of 2 mL DMEM and 2.5% DMSO. Then, 2 mL of fusion solution was added dropwise to the cells before they were incubated for 10 min at 37°C. The fusion solution was then aspirated, 10 mL of standard media was added, and the cells were placed back in the incubator at 37°C overnight. The next day, the fused tsA201 cells were separated from single cells with the use of a 20 μm mesh filter.

Fused cells were cotransfected with both α and β1 subunits on two consecutive days using X-Fect (Clontech, Mountain View, CA). Tetrodotoxin (600 nM) and/or lidocaine hydrochloride (100 μM) were added to the standard culture media of cells because anecdotal evidence suggested that expression levels may be increased. Three to six days after transfection, fused cells were detached from culture dishes with Gibco trypsin-EDTA solution (Life Technologies, Grand Island, NY) and studied electrophysiologically.

Recording technique, solutions, experimental protocols, and analysis

Recordings were made using a large-bore, double-barreled glass suction pipette for both voltage clamp and internal perfusion as previously described (28). Temperature was controlled by means of a Sensortek TS-4 thermoelectric stage (Physitemp Instruments, Clifton, NJ) mounted beneath the bath chambers and varied by <0.5°C. Cells were studied at 13°C.

The control extracellular solution for I_{Na} measurements contained (in mM) 15 Na^+, 185 TMA^+, 4 $CaCl_2$, 200 MES^-, and 10 HEPES (pH 7.2), and the intracellular solution contained 200 TMA^+, 75 F^-, 125 MES^-, 10 EGTA, and 10 HEPES (pH 7.2). For measurement of I_g, the intracellular solution remained unchanged, whereas for the extracellular solution Na^+ was replaced with TMA^+, Cl^- was replaced with MES^-, and 1 μM of STX (Calbiochem, San Diego, CA) was added. Then, 10 mM of lidocaine (Sigma-Aldrich) was added to the STX-containing solution and the pH was adjusted to 7.2. Lidocaine hydrochloride (Sigma-Aldrich) was used when the extracellular test solutions contained Na^+. ApA toxin (Sigma Chemical) was used at a concentration of 1 μM, which is three orders of magnitude greater than the K_D (29,30). Because site-3 toxins unbind slowly from modified Na channels at negative membrane (18), the cells were first exposed to ApA toxin in the presence of 15 mM Na_o while they were pulsed at 1 Hz to −40 mV for 50 ms, for a total of 3–5 min. The cells were then transferred to either the control solution containing 15 mM Na_o (to record I_{Na}) or the STX-containing solution (to record I_g). To wash the ApA toxin from the modified Na channels, we depolarized the cell membrane to 0 mV for at least 5 min before obtaining recordings in the wash solutions (18). Recordings were obtained by means of a PXI-1002 chassis with a PXI-6052 multifunction 16-bit converter using LabView 7.1 (all from National Instruments, Austin, TX), and digitized at 200 kHz (National Instruments).

For measurements of I_{Na}, the membrane holding potential, V_{hp}, was −150 mV and stepped to test potentials from −130 to 20 mV for 50 ms at 1 Hz. Data were capacity corrected using four to eight scaled current responses recorded from voltage steps typically between −150 mV and −180 mV, and leak resistance was calculated as the reciprocal of the linear conductance between −180 mV and −110 mV. The peak I_{Na} was taken as the mean of four data samples clustered around the maximal value of data digitally filtered at 5 kHz and leak corrected by the amount of the calculated time-independent linear leak.

For I_g measurements, the membrane potential was held at −150 mV (or −160 mV) and stepped to test potentials for 25 ms at 1 Hz. The voltage-clamp protocols included four repetitions at each test voltage that were 1/4 of a 60 Hz cycle out of phase to maximize rejection of this frequency and thereby improve the signal/noise ratio. All I_g values were leak corrected by the mean of 2–4 ms of data, usually beginning 8 ms after the change in test potential; capacity corrected by using four to eight scaled current responses to steps between −150 mV and −170 (or −180) mV taken immediately before and after the test steps; and filtered by the inherent response of the voltage-clamp electronics (corner frequency ~100 kHz). Q-V relationships were fit with a simple Boltzmann distribution:

$$Q = Q_{max} \Big/ \left(1 + e^{\left(V_t - V_{1/2}\right)/s}\right), \quad (1)$$

where Q is the charge during the depolarizing step and V_t is the test potential. For the fitted parameters, Q_{max} is the maximum charge, $V_{1/2}$ is the half-point of the relationship, and s is the slope factor in mVs. Fractional Q was calculated as Q/Q_{max}.

For I_{Na} versus Q_{max} plots, the data were fit with a linear equation:

$$Q_{max} = m \times I_{Na} \quad (2)$$

where I_{Na} is the peak current during a test potential to 0 mV, m is the slope, and Q_{max} is the maximal gating charge from a Boltzmann fit to each cell's Q-V relationship.

Data were analyzed and graphed using MATLAB (The MathWorks, Natick, MA) and Origin (OriginLab, Northhampton, MA). Unless otherwise specified, summary statistics are expressed as the means ± 1 standard deviation (SD). The figures show the means ± standard error of the mean (SEM). Both paired and nonpaired Student's *t*-tests (as indicated) were used to determine statistical significance at the $p < 0.05$ level.

RESULTS

Important role of N1764 in DIV

Previous studies on charged substitutions of the Asn in DIV-S6 (see Table 1) in $rNa_V1.4$ by either Asp or Lys showed that I_{Na} expressed well (31). However, a cysteine-scanning mutagenesis study in $rNa_V1.4$ showed that mutant channels with substitution of the Asn by Cys in DIV-S6 expressed no I_{Na}, suggesting poor channel expression (14). A similar study of $rNa_V1.4$ in which the Asn was substituted with an Ala in DIV-S6 showed that the cells expressed very small magnitudes of I_{Na} (14,15). However, another possible explanation for the small magnitudes of I_{Na} in channels with either Cys or Ala substitutions for Asn is that the mutant channels expressed well but produced minimal ion currents. Multiple studies have previously reported that DIV-S4 plays a special role in Na channel kinetics, being strongly associated with fast inactivation from the open state (17,29,32,33). Consequently, a possible explanation for the small magnitudes of I_{Na} after Ala or Cys substitutions for Asn in the DIV-S6 is that the mutant channels expressed well but were not very conductive, possibly because the mutant channels were inactivated. If this were the case, then expression of N1764A or N1764C in $Na_V1.5$ would result in the presence of large Na channel gating currents (I_g) even if the mutant channels had little or no I_{Na}. We transfected the two DIV-S6 mutants of $Na_V1.5$, N1764A and N1764C, into fused mammalian cells and found that both mutant channels expressed well as measured by the presence of gating charge, even though the magnitude of I_{Na} was markedly reduced compared with the WT channels. Fig. 1 plots the magnitude of the peak I_{Na} during a step depolarization to 0 mV versus Q_{max} as determined from Boltzmann fits to their Q-V relationships. Also shown are results for the WT. Note that substitution with Cys resulted in the smallest magnitudes of I_{Na}, and Ala substitution resulted in only a slightly larger magnitude. In contrast, the largest Q_{max} for any of the mammalian cells was recorded in N1764C. These data show that N1764C and N1764A both express well, but the mutations only allow for very small magnitudes of I_{Na}.

Because DIV-S4 appears to be tightly coupled to fast inactivation from the open state in WT channels, it is possible that substitution with Cys or Ala for N1764 in DIV-S6 caused the voltage sensor, DIV-S4, to be in a sustained, depolarized position, leading to channel inactivation. If this were the case, one would anticipate that the mutant

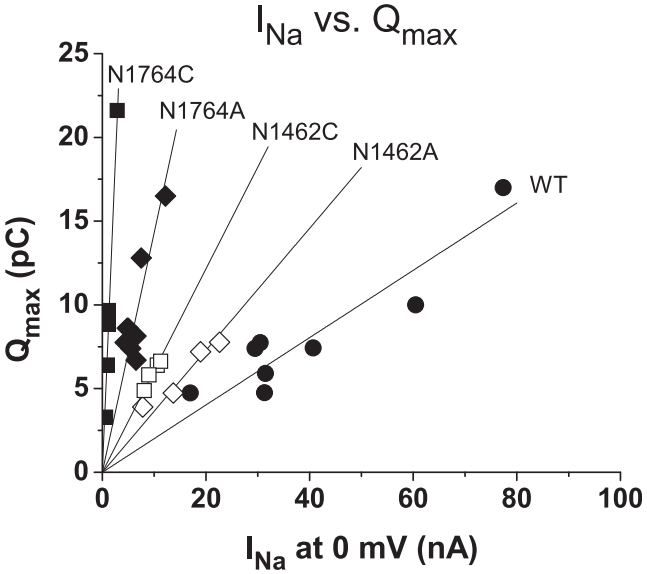

FIGURE 1 Plot of peak I_{Na} versus Q_{max} for Asn substitutions in the S6s of DIII, DIV, and WT $Na_V1.5$. The peak I_{Na} during a step depolarization to 0 mV from a holding potential of −150 mV was plotted against Q_{max} as determined from fits to the Q-V relationships for the WT (●) and the mutant channels N1764C (■), N1764A (◆), N1462C (□), and N1462A (◇). The lines represent the best linear fits to each group of mutant channels (Eq. 2). The slope (pC/nA) for N1764C = 7.39, N1764A = 1.43, N1462C = 0.61, N1462A = 0.36, and WT = 0.20.

Na channels would become rapidly inactivated by having their inactivation gate (formed by intracellular linker between DIII and DIV) bind to its putative receptor if its DIV-S4 were in a depolarized conformation. To test for this possibility, we used the site-3 toxin ApA. In WT cells, ApA toxin has been shown to bind to the S3-S4 extracellular linker of DIV and to inhibit gating charge movement of the DIV-S4 during depolarizing pulses (17,18,20), presumably by maintaining that S4 in a retracted, hyperpolarized position (19). Consequently, if N1764C or N1764A caused the DIV-S4 to assume a stabilized-inactivated position regardless of the membrane potential, exposure of the mutant channel to ApA toxin should have caused little or no change in Q_{max} because the S4 would have already been stabilized by the Asn mutations. Fig. 2 shows an example of ApA toxin modification of the small I_{Na} for N1764A. Note that ApA toxin could still bind to the mutant channel, as indicated by the slowing of I_{Na} decay. Q-V relationships for the mutant channels are shown for N1764A (Fig. 2 *C*) and N1764C (Fig. 2 *D*) before and after exposure to ApA toxin. Note that the toxin caused an ~30% reduction in Q_{max} for both mutant channels, which is similar to what was observed for WT channels (17). These results suggest that DIV-S4 is not stabilized in either N1764A or N1764C, and instead is able to move in response to step depolarizations. Consequently, these results suggest that the Ala and Cys substitutions for N1764 uncouple the voltage-sensor domain from the pore domain.

Uncoupling the voltage-sensor domain from the pore domain in DIV

Previous studies have shown that lidocaine binding to the inner vestibule of the Na channel's pore (4–6) affects movement of the S4s in DIII and DIV through coupling of the channel's pore domain to its voltage-sensor domain (8,12). It was also shown that lidocaine reduces Q_{max} by nearly 38% because of complete stabilization of DIII-S4 in an outward, depolarized position (responsible for ~74% of the total reduction in Q_{max}, or 28%) and by partial stabilization of DIV-S4 in an outward position (contributing the remaining 26% of the total reduction in Q_{max}, or 10%) (8,9). If Ala or Cys substitution of N1764 uncouples the S6 from its S4 in DIV, the actions of lidocaine on gating charge in the

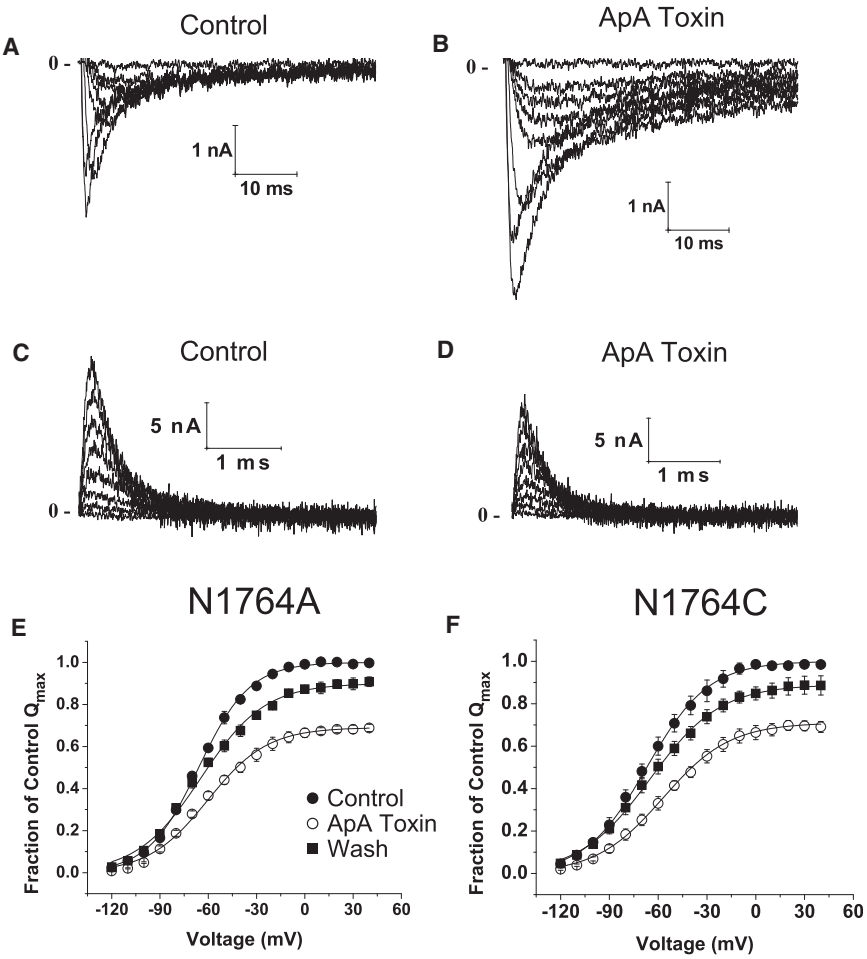

FIGURE 2 Effect of ApA toxin on N1764A and N1764C. (*A* and *B*) I_{Na} recordings of N1764A before (*A*) and after (*B*) 1 μM of ApA toxin for test potentials between −110 and 20 mV from a V_{hp} of −150 mV. (*C* and *D*) I_g recordings of N1764A before (*C*) and after (*D*) 1 μM of ApA toxin for test potentials between −110 and 40 mV from a V_{hp} of −150 mV. (*E*) Q-V relationships for N1764A ($n = 4$ cells) in control, ApA toxin, and wash. The solid lines represent the means of the best fits to the individual cells by a Boltzmann distribution (Eq. 1) where the Q_{max} for each cell was normalized to the fitted Q_{max} value in the control. The legend inset applies to both panels. In the control, the slope factor was 16 ± 2 mV and the $V_{1/2}$ was −66 ± 1 mV, whereas after ApA toxin application the Q_{max} decreased to 0.69 ± 0.03 ($p < 0.05$ compared with control), the slope was 18 ± 2 mV, and the $V_{1/2}$ was −60 ± 5 mV. After washing of the toxin, the Q_{max} increased to 0.90 ± 0.04, the slope was 20 ± 2 mV, and the $V_{1/2}$ was −65 ± 4 mV. (*F*) Q-V relationships for N1764C ($n = 4$ cells) in control, ApA toxin, and wash. In the control, the slope factor was 19 ± 3 mV and the $V_{1/2}$ was −67 ± 7 mV, whereas after ApA toxin application the Q_{max} decreased to 0.71 ± 0.06 ($p < 0.05$ compared with control), the slope was 21 ± 2 mV, and the $V_{1/2}$ was −57 ± 5 mV. After washing of the toxin, the Q_{max} increased to 0.89 ± 0.08, the slope was 21 ± 1 mV, and the $V_{1/2}$ was −65 ± 6 mV.

mutant channels should result in a smaller reduction in the gating charge (~28–30%) compared with the 38% reduction in Q_{max} by lidocaine in WT. To determine the effect of lidocaine on the gating charge of N1764C and N1764A, we exposed cells expressing those channels to 10 mM of extracellular lidocaine. Fig. 3 shows the Q-V relationships for the two mutant channels. Lidocaine decreased Q_{max} by only 26% in N1764A and by only 22% in N1764C. These values are close to the expected reduction in Q_{max} of 28–30% if lidocaine binding to the inner pore of the Na channel could stabilize only DIII-S4, and not DIV-S4, in the mutant channels due to the uncoupling of DIV-S4 from its pore.

Important role of N1462 in DIII

Previous I_{Na} studies on the role of the Asn residue in DIII-S4 in the rat brain IIA $Na_V1.2$ channel showed that N1466A (corresponding to N1462 in $Na_V1.5$) shifted the voltage-dependent inactivation $V_{1/2}$ leftward by approximately −10 mV, with no change in the use-dependent block of I_{Na} by etidocaine (5). In addition, lidocaine binding to the inner pore of WT was shown to produce complete stabilization of DIII-S4, which is responsible for nearly three-fourths of the 38% reduction in Q_{max} by lidocaine (or ~30%, with the other one-fourth resulting from partial stabilization of DIV-S4) in $Na_V1.5$ (8,34). If N1462 plays an important role in coupling the pore domain to the voltage-sensor domain in DIII, then lidocaine binding to the mutant channel should result in a smaller decrease in Q_{max} than the 38% decrease seen in the WT.

Similar to what we observed for $Na_V1.2$ (see above), we found that Ala and Cys substitutions of N1462 in $Na_V1.5$ (N1462A and N1462C, respectively) expressed well, with much larger magnitudes of I_{Na} compared with the DIV Asn mutants (N1764A and N1764C; see Fig. 1). The Q-V relationships for N1462A and N1462C before and after exposure to 10 mM of lidocaine are shown in Fig. 4. Lidocaine reduced the Q_{max} in N1462A by only 13%, whereas it reduced the Q_{max} in N1462C by a little more, 17%. Assuming that lidocaine binding to the pore in the mutant channels caused a partial stabilization of DIV-S4 (as it does in the WT), which would be responsible for an 8% decrease in Q_{max}, N1462A and N1462C demonstrated almost complete uncoupling of DIII-S6 from its S4, causing only a 5% and 9% decrease, respectively, compared with the 30% decrease due to DIII-S4 in the WT.

Effect of lidocaine on N1462A + N1764A in $Na_V1.5$

Because each individual substitution of the Asn in DIII-S6 and DIV-S6 by Ala markedly reduced the coupling of the pore domain to the voltage-sensor domain in $Na_V1.5$, the double Ala substitution, N1462A + N1764A, should show almost no reduction in Q_{max} by lidocaine if the effects of the mutations are additive. Fig. 5 shows that this is the case. When both DIII and DIV Asn residues were substituted with Ala, lidocaine caused no significant decrease in Q_{max}, with only a small shift in $V_{1/2}$ and a small change in the slope factor. As expected, we found that the I_{Na} magnitude was too small to be reliably measured in the double mutation (data not shown).

Effects of Ala substitutions for Asn in the rat $Na_V1.4$ channel

To determine whether Asn residues in the two S6s of $Na_V1.5$ have effects generalizable to other Na_V channels, we investigated the roles of Asn in $rNa_V1.4$ expressed with the $\beta1$ subunit. First, we confirmed the effect of 10 mM of lidocaine on the Q-V relationship of WT $rNa_V1.4$ expressed with the $\beta1$ subunit. Fig. 6 shows that lidocaine had a nearly identical effect on the $Na_V1.4$ Q-V relationship compared

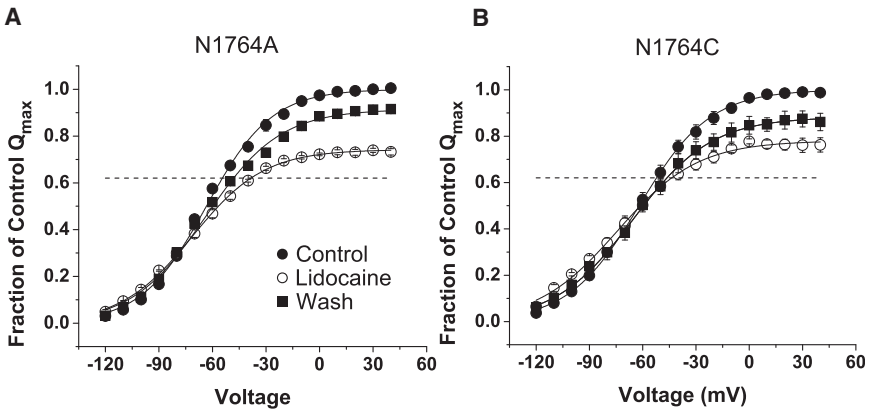

FIGURE 3 Effect of lidocaine on the Q_{max} of N1764A and N1764C. (*A*) Q-V relationships in $Na_V1.5$ for N1764A ($n = 4$ cells) in control, 10 mM lidocaine, and wash. The solid lines represent the means of the best fits to the individual cells by a Boltzmann distribution (Eq. 1) where the Q_{max} for each cell was normalized to the fitted Q_{max} value in the control. The dashed line represents the 38% reduction in Q_{max} by 10 mM lidocaine in WT channels (8). The legend inset applies to both panels. Lidocaine (10 mM) blocked all I_{Na} in one N1764A cell (data not shown). In the control, the slope factor was 18 ± 2 mV and the $V_{1/2}$ was −63 ± 1 mV, whereas in lidocaine the Q_{max} decreased to 0.74 ± 0.02 ($p < 0.05$ compared with control), the slope was 20 ± 2 mV ($p < 0.05$), and the $V_{1/2}$ was −71 ± 3 mV ($p < 0.05$). After washing, the Q_{max} increased to 0.91 ± 0.02, the slope was 21 ± 1 mV, and the $V_{1/2}$ was −64 ± 1 mV. (*B*) Q-V relationships for N1764C ($n = 4$ cells) in control, 10 mM lidocaine, and wash. In the control, the slope factor was 20 ± 2 mV and the $V_{1/2}$ was −62 ± 6 mV, whereas in lidocaine the Q_{max} decreased to 0.78 ± 0.04 ($p < 0.05$ compared with control), the slope was 23 ± 2 mV (<0.05), and the $V_{1/2}$ was −74 ± 3 mV ($p < 0.05$). After washing, Q_{max} increased to 0.88 ± 0.07, the slope was 22 ± 2 mV, and the $V_{1/2}$ was −65 ± 3 mV.

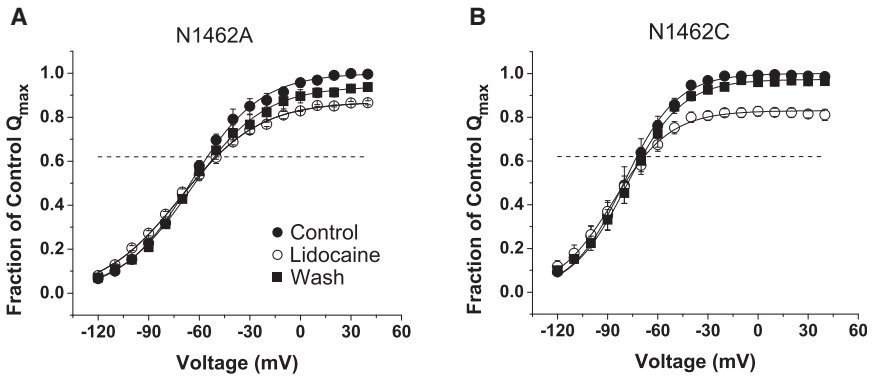

FIGURE 4 Effect of lidocaine on the Q_{max} of N1462A and N1462C. (*A*) Q-V relationships in $Na_V1.5$ for N1462A ($n = 4$ cells) in control, 10 mM lidocaine, and wash. The solid lines represent the means of the best fits to the individual cells by a Boltzmann distribution (Eq. 1) where the Q_{max} for each cell was normalized to the fitted Q_{max} value in the control. The dashed line represents the 38% reduction in Q_{max} by 10 mM lidocaine in WT channels (8). The legend inset applies to both panels. In the control, the slope factor was 21 ± 4 mV and the $V_{1/2}$ was −65 ± 3 mV, whereas in lidocaine the Q_{max} decreased to 0.87 ± 0.02 ($p < 0.05$ compared with control), the slope was 23 ± 2 mV, and the $V_{1/2}$ was −71 ± 5 mV ($p < 0.05$). After washing, the Q_{max} increased to 0.94 ± 0.03, the slope was 22 ± 5 mV, and the $V_{1/2}$ was −65 ± 4 mV. (*B*) Q-V relationships for N1462C ($n = 4$ cells) in control, 10 mM lidocaine, and wash. In the control, the slope factor was 16 ± 1 mV and the $V_{1/2}$ was −80 ± 9 mV, whereas in lidocaine the Q_{max} decreased to 0.83 ± 0.04 ($p < 0.05$ compared with control), the slope was 17 ± 2 mV ($p = 0.052$), and the $V_{1/2}$ was −68 ± 8 mV ($p < 0.05$). After washing, the Q_{max} increased to 0.97 ± 0.01, the slope was 17 ± 2 mV, and the $V_{1/2}$ was −78 ± 7 mV.

with $Na_V1.5$, with a decrease in Q_{max} of 36% accompanied by a characteristic leftward shift in $V_{1/2}$ and a more shallow slope.

Substitution of Asn by Ala or Cys in the DIV-S6 of $rNa_V1.4$ (N1584A and N1584C, respectively) resulted in mutant channels that expressed well as measured by gating currents, but both mutants had very small I_{Na} magnitudes similar to what was observed for the $Na_V1.5$ mutants. The inset in Fig. 7 *A* shows the plot of I_{Na} at 0 mV versus Q_{max} for both mutations on the same scale shown in Fig. 1. The slope for both mutations was 5.3 pC/nA, which is similar to the value found for N1764C in $Na_V1.5$. In the presence of lidocaine, Q_{max} was decreased by 27% in N1584A (Fig. 7 *A*) and by 24% in N1584C (Fig. 7 *B*), versus

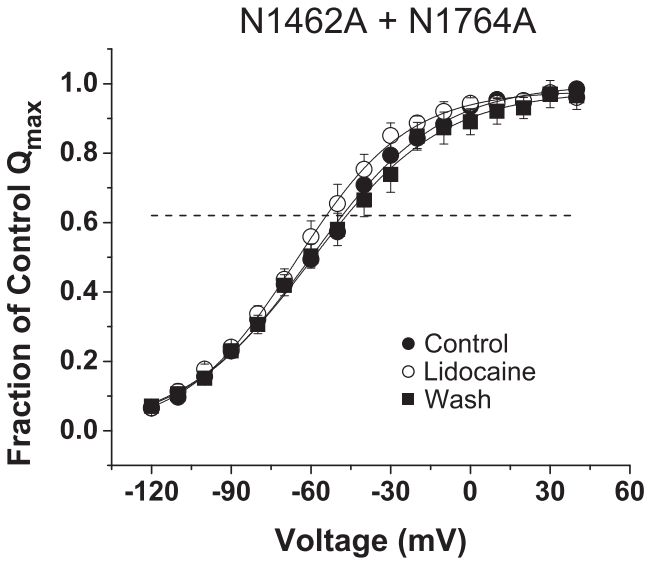

FIGURE 5 Effect of lidocaine on the Q_{max} of $Na_V1.5$ N1462A + N1764C. Q-V relationships in $Na_V1.5$ for the double substitution in $Na_V1.5$, N1462A + N1764C ($n = 4$ cells) in control, 10 mM lidocaine, and wash. The solid lines represent the means of the best fits to the individual cells by a Boltzmann distribution (Eq. 1) where the Q_{max} for each cell was normalized to the fitted Q_{max} value in the control. The dashed line represents the 38% reduction in Q_{max} by 10 mM lidocaine in WT channels (8). In the control, the slope factor was 24 ± 3 mV and the $V_{1/2}$ was −60 ± 4 mV. In lidocaine, Q_{max} did not decrease significantly ($Q_{max} = 0.98 \pm 0.03$). However, both the $V_{1/2}$ (−65 ± 6 mV) and the slope factor (21 ± 3 mV) were significantly different in lidocaine. After washing, the Q_{max} was 0.98 ± 0.06, the slope was 25 ± 2 mV, and the $V_{1/2}$ was −60 ± 5 mV.

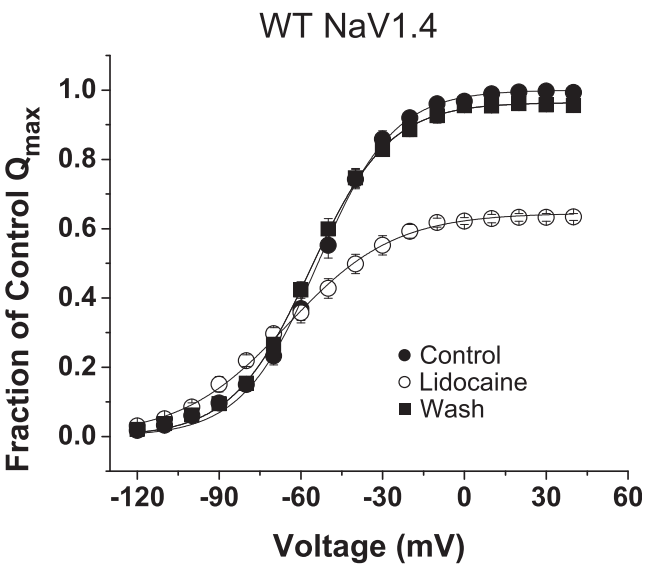

FIGURE 6 Effect of lidocaine on the Q-V relationship in $rNa_V1.4$ WT channels. Q-V relationships for $rNa_V1.4$ WT ($n = 5$ cells) were constructed in control solution, 10 mM lidocaine, and wash. The solid lines represent the means of the best fits to the individual cells by a Boltzmann distribution (Eq. 1) where the Q_{max} for each cell was normalized to the fitted Q_{max} value in the control. In the control, the slope factor was 14 ± 1 mV and the $V_{1/2}$ was −54 ± 5 mV. In lidocaine, Q_{max} decreased to 0.64 ± 0.03, the slope factor was 20 ± 2 mV, and the $V_{1/2}$ was −65 ± 8 mV (all three measurements were significantly different from control). After washing, the Q_{max} increased by 0.96 ± 0.04, the slope was 14 ± 2 mV, and the $V_{1/2}$ was −57 ± 3 mV.

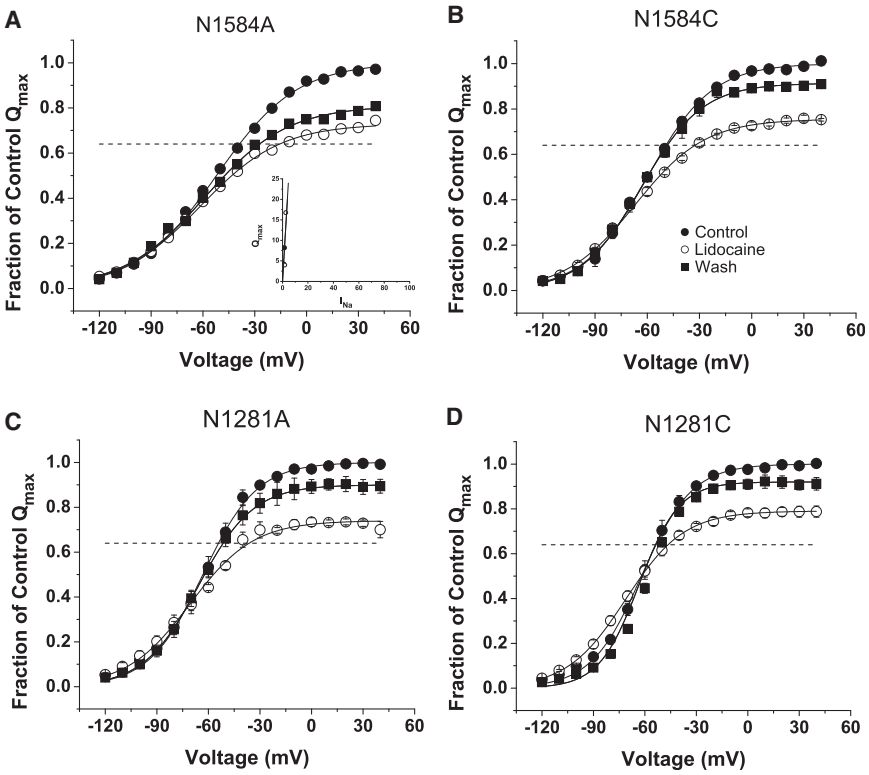

FIGURE 7 Effect of lidocaine on the Q-V relationships in rNa$_V$1.4 mutant channels. (*A*) Q-V relationships for rNa$_V$1.4 N1584A ($n = 2$ cells) were constructed in control solution, 10 mM lidocaine, and wash. The solid lines represent the means of the best fits to the individual cells by a Boltzmann distribution (Eq. 1) where the Q_{max} for each cell was normalized to the fitted Q_{max} value in the control. The dashed line represents the 36% reduction in Q_{max} by 10 mM lidocaine seen in WT rNa$_V$1.4. The inset in (*A*) shows the plots of peak I_{Na} (0 mV) versus Q_{max} for the mutations N1584A (○) and N1584C (●) on the same scale as in Fig. 1, where the slope for both N1584C and N1584A was 5.3 pC/nA. The inset in (*B*) applies to all panels. In the control, the slope factor was 23 ± 5 mV and the $V_{1/2}$ was −52 ± 5 mV. In lidocaine, Q_{max} decreased to 0.73 ± 0.05 ($p = 0.09$), the slope factor was 23 ± 2 mV, and the $V_{1/2}$ was −62 ± 1. After washing, the Q_{max} increased 0.80 ± 0.05, the slope was 24 ± 6 mV, and the $V_{1/2}$ was −59 ± 4 mV. (*B*) Q-V relationships are shown for rNa$_V$1.4 N1584C ($n = 3$ cells). In the control, the slope factor was 18 ± 2 mV and the $V_{1/2}$ was −60 ± 2 mV. In lidocaine, Q_{max} decreased to 0.76 ± 0.02 ($p < 0.05$), the slope factor was 20 ± 1 mV, and the $V_{1/2}$ was −67 ± 2. After washing, the Q_{max} increased 0.91 ± 0.02, the slope was 17 ± 2 mV, and the $V_{1/2}$ was −63 ± 3 mV. (*C*) Q-V relationships are shown for rNa$_V$1.4 N1281A ($n = 4$ cells). In the control, the slope factor was 16 ± 1 mV and the $V_{1/2}$ was −63 ± 5 mV. In lidocaine, Q_{max} decreased to 0.74 ± 0.02 ($p < 0.05$), the slope factor was 19 ± 1 mV ($p < 0.05$), and the $V_{1/2}$ was −71 ± 6. After washing, the Q_{max} increased 0.90 ± 0.07, the slope was 16 ± 3 mV, and the $V_{1/2}$ was −66 ± 4 mV. (*D*) Q-V relationships are shown for rNa$_V$1.4 N1281C ($n = 3$ cells). In the control, the slope factor was 15 ± 1 mV and the $V_{1/2}$ was −62 ± 4 mV. In lidocaine, Q_{max} decreased to 0.79 ± 0.04 ($p < 0.05$), the slope factor was 17 ± 2 mV, and the $V_{1/2}$ was −71 ± 6. After washing, the Q_{max} increased 0.92 ± 0.04, the slope was 12 ± 6 mV, and the $V_{1/2}$ was −63 ± 5 mV.

36% in WT channels (Fig. 6). These decreases in the Q_{max} of N1584A and N1584C after exposure to lidocaine were similar in magnitude to the corresponding mutations in NaV1.5 (see Fig. 3).

Substitutions of the Asn in DIII-S6 by Ala and Cys (N1281A and N1281C, respectively) in rNa$_V$1.4 appeared to produce less uncoupling than the equivalent mutations in Na$_V$1.5. Fig. 7 *C* shows that lidocaine reduced Q_{max} in N1281A in rNa$_V$1.4 by 26%, a value greater than the 13% decrease by lidocaine seen in the equivalent mutant channel in Na$_V$1.5 (N1462A; see Fig. 4 *A*). A decrease of 21% in Q_{max} by lidocaine was also found for N1281C in rNa$_V$1.4. Results for both N1281A and N1281C suggest that the substitutions for the Asn in DIII-S6 were able to maintain a greater degree of coupling between its pore domain and voltage-sensor domain in rNa$_V$1.4 compared with the equivalent substitutions in Na$_V$1.5.

DISCUSSION

We have shown that conserved Asn residues in the S6s of DIII and DIV (see Table 1) in Na$_V$1.5 have an important role in coupling the pore domain to the voltage-sensor domain, as measured by the actions of lidocaine. Substitution of the Asn residue by either Cys or Ala in DIV-S6 appears to completely uncouple the pore domain from its voltage-sensor domain. Although it is possible that lidocaine binding to the Na channel pore may distort the channel's structure compared with the unbound WT channel, the apparent uncoupling of the pore domain from the voltage-sensor domain in the nondrug-bound channel can be inferred for N1764C and N1764A because they exhibit very small I_{Na} magnitudes even though they express well as measured by gating currents. Given the special role played by DIV-S4 in fast inactivation (17,29,32,33), the dichotomy of small I_{Na} magnitudes in the presence of large gating currents could be a result of the mutant channels becoming inactivated because the voltage-dependent DIV-S4 is no longer able to act upon its DIV-S6. The finding that the site-3 toxin ApA reduced Q_{max} in both N1764C and N1764A by ~30% (see Fig. 2), the same amount as in WT Na$_V$1.5 (17–19), confirms that DIV-S4 was not stabilized by the Asn substitutions and continued to move as a function of the membrane potential.

In Na$_V$1.5, substitution of either an Ala or Cys for N1462 in DIII-S6 also uncoupled the pore domain from

the voltage-sensor domain. However, the uncoupling may be more complete for an Ala substitution compared with a Cys substitution because the decrease in Q_{max} by lidocaine was smaller in N1462A (13%) than in N1462C (17%) (Fig. 4). Even though the substitutions of Ala and Cys for Asn are generally considered to be conservative and are not thought to typically disrupt α-helices, and do not have a large side-chain volume that could disrupt protein-protein interactions, nonspecific effects on the channel cannot be ruled out. The almost complete lack of a decrease in Q_{max} by lidocaine in the double mutation of $Na_V1.5$, N1462A + N1764A, where both Asn residues in the S6s of DIII and DIV were substituted (see Fig. 5), suggests that each mutation acts independently, i.e., their effects are additive. Because the double mutation has such small magnitudes of I_{Na} and lidocaine has minimal effects on the Q-V relationship, it is possible that lidocaine does not have the ability to bind to the mutant channel. Although that is a possible explanation, it is unlikely because the Asn residues are not thought to form part of the lidocaine-binding site (4–7), and lidocaine can bind to channels with each individual mutation. Lastly, the Q-V relationship for the double-mutant channel shows a small, significant leftward shift in lidocaine compared with its control, further suggesting that lidocaine can still bind to the mutant channel.

Comparison with $Na_V1.4$

To determine whether our findings for Asn substitutions are generalizable to other Na channel isoforms, we repeated many of the Asn substitutions at equivalent positions in $rNa_V1.4$. Initially, we showed that lidocaine decreased the Q_{max} of WT $rNa_V1.4$ by 36%, an amount comparable to that observed in WT $Na_V1.5$, suggesting that the S4s in DIII and DIV in WT $rNa_V1.4$ contribute the same fraction of gating charge to its Q_{max} as does $Na_V1.5$. This is consistent with the previous finding that the DIV-S4s in both Na channel isoforms contribute the same fraction of gating charge to the Q_{max} (35). The individual Ala or Cys substitutions in the DIV-S6 of $rNa_V1.4$ appear to behave similarly to those in $Na_V1.5$: either substitution appears to almost completely uncouple the pore domain from the voltage-sensor domain, because the Q_{max} in lidocaine is decreased by only 24–27% (Fig. 7, *A* and *B*), an amount of decrease that is consistent with stabilization of the S4 in DIII, but not DIV-S4 (8).

Ala or Cys substitutions for the Asn in DIII-S6 appear to have a smaller effect on uncoupling in $rNa_V1.4$ than in $Na_V1.5$. In the mutants N1281A and N1281C ($rNa_V1.4$), lidocaine caused the Q_{max} to be reduced by 21–26%, compared with a 13% reduction in N1462A (in $Na_V1.5$), which suggests that there is only a partial uncoupling in the mutant $rNa_V1.4$ channels. Our finding that the asparagine mutants in NaV1.4 DIII-S6 exhibit less uncoupling between the voltage-sensor domain and pore domain compared with homologous mutants in NaV1.5 is supported by previous studies that measured shifts in the fluorescence-voltage curves of DIII-S4 in $rNa_V1.4$ expressed in *Xenopus* ooctyes (12,13).

Implications for a molecular model of the voltage-gated Na channel

If the crystal structures of voltage-gated channels, including the Kv1.2 channel (3) and the bacterial Na channels Na_VAb (36) and Na_VMs (37), are applicable to the voltage-gated mammalian Na channel, the coupling between any single pore domain and its voltage-sensor domain would involve its corresponding S4-S5 linker acting downstream upon its S6. Depolarization would be expected to result in outward translocation of the S4s, which would permit the S6 segments to hinge open, leading to opening of the pore, presumably by conformational changes in the S6s. These same structures have been modeled to create a channel conformation containing the S6 segments of the Na channel, with the S6 segments in DIII and DIV making the most important contributions to the high-affinity lidocaine-binding site (4–6). Local anesthetic-binding sites have also been described for the bacterial Na channels (38,39). Due to movement of the S4s in DIII and DIV during depolarization, downstream effects on their S6 segments result in the creation of a high-affinity lidocaine-binding site. During repolarization, the voltage sensors in DIII and DIV would have the opposite effect: their movement back to an inward, rested position would bias the S6 segments toward a closed position, thereby decreasing lidocaine's affinity. The results reported here suggest that the Asn residues in the S6s of DIII and DIV are important for coupling the pore domain to the voltage-sensor domain. It should be noted that other residues contained in the DIII S4-S5 linker and the S5 or S6 helices also affect the coupling of the DIII-S4 voltage sensor to its pore (12,13). Molecular modeling studies of the pore domain of the voltage-gated Na channel place the conserved Asn residues intracellularly at a position that is two residues inward from the putative bundle crossing in $Na_V1.5$ (6). The intracellular position of the Asn residues represents another locus for interaction between the voltage-sensor and pore domains in addition to that previously reported for coupling of the outer pore of the Na channel to its voltage sensor in DIV (11). The intracellular position of the Asn residues contrasts with previously reported coupling of the outer pore of the Na channel to the voltage sensor in DIV (11). We have shown that substitution by Ala or Cys decouples the pore and voltage-sensor domains; however, neither substitution would be expected to alter the presumed α-helix of the S6 segments. Consequently, the uncoupling by either Ala or Cys substitutions of Asn suggests that the interaction between the S4-S5 linker and its S6 may be more involved than just blocking the movement of the S6 segment. Although the bacterial Na channels, Na_VAb and Na_VMs,

are composed of four homologous tetramers, in contrast to mammalian voltage-gated Na channels with an α-subunit, both Na_VAb (40) and Na_VMs (37) have an Asn in their S6s in a location similar to that observed in $Na_V1.5$, suggesting that the Asn residues may have an important role in coupling the pore domain to the voltage-sensor domain in bacterial Na channels as well.

In the Shaker K channel, the S6 segments appear to open passively when their S4s are in a depolarized position (41). This may be the case for Na channels as well (at least for DIV-S6) because they behave as though they are in an inactivated state in N1764A and N1764C, presumably because the DIV-S6 has assumed a depolarized open position that facilitates inactivation and binding of the putative inactivation gate. Although we did not investigate the roles of the conserved Asn residues in the S6 segments of DI and DII, it would not be unexpected to find that these residues are also important for coupling their pore domains to their voltage-sensor domains.

In summary, we have shown that the Asn residues in the S6 segments of DIII and DIV play an important role in coupling the actions of their voltage-sensor domains to their pore domains.

AUTHOR CONTRIBUTIONS

Experimental rationale and design: D.A.H., H.A.F., and M.F.S. Experiments and data analysis: M.F.S. Manuscript preparation: D.A.H. and M.F.S.

ACKNOWLEDGMENTS

We are grateful to WenQing Yu, MD, for her excellent technical assistance.

The experiments in this work were supported by the Nora Eccles Treadwell Foundation.

REFERENCES

1. Catterall, W. A. 2000. From ionic currents to molecular mechanisms: the structure and function of voltage-gated sodium channels. *Neuron.* 26:13–25.
2. Jiang, Y., A. Lee, …, R. MacKinnon. 2003. X-ray structure of a voltage-dependent K+ channel. *Nature.* 423:33–41.
3. Long, S. B., E. B. Campbell, and R. Mackinnon. 2005. Crystal structure of a mammalian voltage-dependent Shaker family K+ channel. *Science.* 309:897–903.
4. Ragsdale, D. S., J. C. McPhee, …, W. A. Catterall. 1994. Molecular determinants of state-dependent block of Na+ channels by local anesthetics. *Science.* 265:1724–1728.
5. Yarov-Yarovoy, V., J. Brown, …, W. A. Catterall. 2001. Molecular determinants of voltage-dependent gating and binding of pore-blocking drugs in transmembrane segment IIIS6 of the Na(+) channel alpha subunit. *J. Biol. Chem.* 276:20–27.
6. Lipkind, G. M., and H. A. Fozzard. 2005. Molecular modeling of local anesthetic drug binding by voltage-gated sodium channels. *Mol. Pharmacol.* 68:1611–1622.
7. Hanck, D. A., E. Nikitina, …, M. F. Sheets. 2009. Using lidocaine and benzocaine to link sodium channel molecular conformations to state-dependent antiarrhythmic drug affinity. *Circ. Res.* 105:492–499.
8. Sheets, M. F., and D. A. Hanck. 2003. Molecular action of lidocaine on the voltage sensors of sodium channels. *J. Gen. Physiol.* 121:163–175.
9. Sheets, M. F., T. Chen, and D. A. Hanck. 2011. Lidocaine partially depolarizes the S4 segment in domain IV of the sodium channel. *Pflugers Arch.* 461:91–97.
10. Muroi, Y., and B. Chanda. 2009. Local anesthetics disrupt energetic coupling between the voltage-sensing segments of a sodium channel. *J. Gen. Physiol.* 133:1–15.
11. Capes, D. L., M. Arcisio-Miranda, …, B. Chanda. 2012. Gating transitions in the selectivity filter region of a sodium channel are coupled to the domain IV voltage sensor. *Proc. Natl. Acad. Sci. USA.* 109:2648–2653.
12. Arcisio-Miranda, M., Y. Muroi, …, B. Chanda. 2010. Molecular mechanism of allosteric modification of voltage-dependent sodium channels by local anesthetics. *J. Gen. Physiol.* 136:541–554.
13. Muroi, Y., M. Arcisio-Miranda, …, B. Chanda. 2010. Molecular determinants of coupling between the domain III voltage sensor and pore of a sodium channel. *Nat. Struct. Mol. Biol.* 17:230–237.
14. Sunami, A., A. Tracey, …, H. A. Fozzard. 2004. Accessibility of midsegment domain IV S6 residues of the voltage-gated Na+ channel to methanethiosulfonate reagents. *J. Physiol.* 561:403–413.
15. Wang, G. K., C. Quan, and S. Wang. 1998. A common local anesthetic receptor for benzocaine and etidocaine in voltage-gated mu1 Na+ channels. *Pflugers Arch.* 435:293–302.
16. Makielski, J. C., B. Ye, …, M. J. Ackerman. 2003. A ubiquitous splice variant and a common polymorphism affect heterologous expression of recombinant human SCN5A heart sodium channels. *Circ. Res.* 93:821–828.
17. Sheets, M. F., and D. A. Hanck. 1995. Voltage-dependent open-state inactivation of cardiac sodium channels: gating current studies with Anthopleurin-A toxin. *J. Gen. Physiol.* 106:617–640.
18. Sheets, M. F., J. W. Kyle, …, D. A. Hanck. 1999. The Na channel voltage sensor associated with inactivation is localized to the external charged residues of domain IV, S4. *Biophys. J.* 77:747–757.
19. Hanck, D. A., and M. F. Sheets. 2007. Site-3 toxins and cardiac sodium channels. *Toxicon.* 49:181–193.
20. Campos, F. V., B. Chanda, …, F. Bezanilla. 2008. Alpha-scorpion toxin impairs a conformational change that leads to fast inactivation of muscle sodium channels. *J. Gen. Physiol.* 132:251–263.
21. Higuchi, R., B. Krummel, and R. K. Saiki. 1988. A general method of in vitro preparation and specific mutagenesis of DNA fragments: study of protein and DNA interactions. *Nucleic Acids Res.* 16:7351–7367.
22. Ho, S. N., H. D. Hunt, …, L. R. Pease. 1989. Site-directed mutagenesis by overlap extension using the polymerase chain reaction. *Gene.* 77:51–59, (see comments).
23. Hartmann, H. A., A. A. Tiedeman, …, G. E. Kirsch. 1994. Effects of III-IV linker mutations on human heart Na^+ channel inactivation gating. *Circ. Res.* 75:114–122.
24. Trimmer, J. S., S. S. Cooperman, …, G. Mandel. 1989. Primary structure and functional expression of a mammalian skeletal muscle sodium channel. *Neuron.* 3:33–49.
25. Satin, J., J. W. Kyle, …, R. B. Rogart. 1992. A mutant of TTX-resistant cardiac sodium channels with TTX-sensitive properties. *Science.* 256:1202–1205.
26. McClatchey, A. I., S. C. Cannon, …, J. F. Gusella. 1993. The cloning and expression of a sodium channel beta 1-subunit cDNA from human brain. *Hum. Mol. Genet.* 2:745–749.
27. Satin, J., J. W. Kyle, …, J. C. Makielski. 1994. Post-repolarization block of cloned sodium channels by saxitoxin: the contribution of pore-region amino acids. *Biophys. J.* 66:1353–1363.
28. Sheets, M. F., J. W. Kyle, …, D. A. Hanck. 1996. Optimization of a mammalian expression system for the measurement of sodium channel gating currents. *Am. J. Physiol.* 271:C1001–C1006.
29. Hanck, D. A., and M. F. Sheets. 1995. Modification of inactivation in cardiac sodium channels: ionic current studies with Anthopleurin-A toxin. *J. Gen. Physiol.* 106:601–616.

30. Khera, P. K., G. R. Benzinger, …, K. M. Blumenthal. 1995. Multiple cationic residues of anthopleurin B that determine high affinity and channel isoform discrimination. *Biochemistry.* 34:8533–8541.

31. Wang, S. Y., and G. K. Wang. 1999. Batrachotoxin-resistant Na+ channels derived from point mutations in transmembrane segment D4-S6. *Biophys. J.* 76:3141–3149.

32. Yang, N., and R. Horn. 1995. Evidence for voltage-dependent S4 movement in sodium channels. *Neuron.* 15:213–218.

33. Chanda, B., and F. Bezanilla. 2002. Tracking voltage-dependent conformational changes in skeletal muscle sodium channel during activation. *J. Gen. Physiol.* 120:629–645.

34. Sheets, M. F., H. A. Fozzard, …, D. A. Hanck. 2010. Sodium channel molecular conformations and antiarrhythmic drug affinity. *Trends Cardiovasc. Med.* 20:16–21.

35. Sheets, M. F., and D. A. Hanck. 1999. Gating of skeletal and cardiac muscle sodium channels in mammalian cells. *J. Physiol.* 514:425–436.

36. Payandeh, J., T. Scheuer, …, W. A. Catterall. 2011. The crystal structure of a voltage-gated sodium channel. *Nature.* 475:353–358.

37. McCusker, E. C., C. Bagnéris, …, B. A. Wallace. 2012. Structure of a bacterial voltage-gated sodium channel pore reveals mechanisms of opening and closing. *Nat. Commun.* 3:1102.

38. Lee, S., S. J. Goodchild, and C. A. Ahern. 2012. Local anesthetic inhibition of a bacterial sodium channel. *J. Gen. Physiol.* 139:507–516.

39. Boiteux, C., I. Vorobyov, …, T. W. Allen. 2014. Local anesthetic and antiepileptic drug access and binding to a bacterial voltage-gated sodium channel. *Proc. Natl. Acad. Sci. USA.* 111:13057–13062.

40. Tikhonov, D. B., and B. S. Zhorov. 2012. Architecture and pore block of eukaryotic voltage-gated sodium channels in view of NavAb bacterial sodium channel structure. *Mol. Pharmacol.* 82:97–104.

41. Kitaguchi, T., M. Sukhareva, and K. J. Swartz. 2004. Stabilizing the closed S6 gate in the Shaker Kv channel through modification of a hydrophobic seal. *J. Gen. Physiol.* 124:319–332.